The Effect of Wave Induced Turbulence on the Rate of Absorption of Gases in Falling Liquid Films

J. C. JEPSEN, O. K. CROSSER, and R. H. PERRY

University of Oklahoma, Norman, Oklahoma

Concentration profiles for carbon dioxide diffusion into thin water films with waves flowing down an inclined plate have been determined. Film Reynolds numbers were varied from 732 to 1,834 at a cell angle of inclination of 9 deg. 44 min. Total diffusivities measured from the concentration profiles showed a marked increase in the central region of the film, with the diffusivity tending toward the molecular diffusivity at the boundaries of the film. Interferometer pictures of the concentration profile showed that the effect of the waves was to compress and expand the profile as the surface of the film changed, but indicated no direct effect on the variation of eddy diffusivity normal to the liquid surface.

Early studies of mass transport from gases into liquids flowing down plates or through packed towers utilized the wetted-wall column to examine the fundamental process of interphase transfer. The main purpose of such a simple apparatus was to permit a precise value for the area across which the transfer occurred. It was noticed that the surface of the film developed ripples at even moderate flows ($N_{Re_L} = 25$) and that the mass transfer was considerably increased above that predicted from theory (*14*; see also *10*, *16*, *29*, and *31*). Considerable effort has been devoted to the explanation of such experimental results, largely with the intention of providing better understanding of the dynamics of the flowing film in the hope that this would lead to a better understanding of the mass transfer results. These studies have established the flow conditions which will cause the ripples to form, the velocity profile in the film, and the increased surface area which results from the presence of the waves.

Flow conditions at which waves form have been studied with some detail. The values for the minimum critical Reynolds number at which waves form quoted in the literature vary, but in general they are small. Binnie (*4*, *5*) reported a value of 4.7 for the critical Reynolds number, Friedman and Miller (*15*) a value of 25, and Brauer (*7*) a value of 8.

More recently, experimental investigations have been made to elucidate the structure of the wave flow. Tailby and Portalski (*35*) measured instantaneous film thicknesses on a 21-in. wide vertical plate with a small capacitance probe. Increases in the surface area as a result of the waves were estimated for this data. Their results showed that at a Reynolds number of 1,000, the surface area was increased by 20%.

Grimley (*17*) measured velocity profiles in films flowing on vertical walls with a modified ultramicroscope. He concluded that the maximum velocity did not occur at the interface, but slightly inward from the surface. Wilkes and Nedderman (*37*) measured velocity profiles in falling films for liquid Reynolds number up to 1.07 by photographing stereoscopically tiny air bubbles in the liquid. They were able to verify Nusselt's parabolic profile under conditions of no waviness and to get average profiles in wavy flow. The shape of the velocity profiles under the condition of waves was still nearly parabolic.

Several theoretical models have been proposed to explain the effect of waves on the mass transfer rate. Danckwerts (*11*) proposed a surface renewal model in which the surface of the liquid film was continually being replaced by fresh liquid. Harriott (*18*) proposed a model for mass transfer from a turbulent fluid to an interface in which eddies arriving at random times come to within random distances from the surface, sweeping away the accumulated solute. Transfer was assumed to be by molecular diffusion in the interval between eddies. Brauer (*7*) assumed that the main resistance to mass transfer was in a laminar layer of liquid next to the wall and that mass transfer in this region was only by molecular diffusion. The thickness of the layer was defined in terms of wall shear stresses which he determined from the experimental film thickness. Stirba and Hurt (*34*) proposed that the effect of waves could be expressed in terms of an eddy diffusion coefficient. Using the analytical solution of Johnstone and Pigford (*21*) for the case of molecular diffusion of a gas into laminar film, they assumed that the thickness of the film with waves was the laminar film thickness and calculated the diffusion coefficient which predicted the experimental values for the average solute concentration in the film. Levich (*27*) used theoretical equations for the velocity components perpendicular and parallel to the direction of flow of the film to obtain equations for the mass transfer of gas into a laminar liquid film with waves. In this analysis he considered bulk flow both perpendicular and parallel to the direction of flow and molecular diffusion from the interface toward the wall. Results of his analysis indicated that the flux into the film was increased by 15% over that expected with laminar flow. The turbulent flow regime was also examined. In this regime Levich assumed that the main mechanism for transfer was turbulence, which he de-

J. C. Jepsen is at Shell Development Company, Emeryville, California. R. H. Perry is at the University of Rochester, Rochester, New York.

scribed as an eddy diffusivity. He assumed that the eddy diffusivity was a maximum in the center of the film and decreased as the wall and free surface were approached.

A critical analysis of these models has not been possible to date because of the lack of experimental data on the concentration profiles in the film. The mass transfer measurements that have been made indicate that all of these models are possible, but selection among them is not feasible.

Results of the experimental and theoretical studies indicated that the waves that form on the surface of a falling film are a symptom of a dynamic action which enhances the mass transfer. In most cases some sort of modification near the surface of the film is postulated which steepens the concentration profile. However, the relationship between the ripple and the dynamic action which enhances the rate of mass transfer is not known. Ideal waves on the surface of a quiet pool do not increase the mass transfer rate (except for the change in surface area); thus the increase in the mass transfer rate in the flowing system must result from some other mechanism of which the waves are a result.

The purpose of the work presented here was to measure experimentally concentration profiles in the film and from this data to determine the value of the eddy diffusivity as a function of location in the film. Amplitude and frequency of the waves on the film were measured so that the mass transfer characteristics might be related to the outward appearance of the film. Details of the construction of the experimental equipment and data not presented in this paper will be found in the original thesis (*22*).

APPARATUS AND PROCEDURE

Measurement of Concentration Profiles

Concentration profile determinations with carbon dioxide transferring into water films were made with a Mach Zehnder interferometer. The measurements were based on the change in index of refraction of the liquid film as gas was absorbed. The carbon dioxide-water system was chosen because the index of refraction was directly proportional to the carbon dioxide concentration, and the heat of solution was negligible.

The theory of the interferometer and application has been discussed in many publications (*2, 3, 8, 9, 13, 19, 23, 26, 28, 30, 33, 36, 38, 39*). Of these, the discussion by Landenburg (*26*) probably is the most informative.

The connecting cell was rectangular in shape with an internal width of 2.95 in., height of 7/16 in., and length of 35.33 in. It was constructed from aluminum with a 1/16-in. thick glass plate 2.95 in. × 34.83 in. cemented to the bottom to act as the surface for the water flow. The sides of the cell were optically flat glass windows 1 in. × 0.4 in. × 36 in. made from shadow graph quality crown glass with a surface accuracy of ¼ wave green light with surfaces parallel to within 30 sec. of arc along any 2-in. section.

The cell was mounted to the rotating base of the interferometer so that the cell could be placed at any angle of inclination between 0 and 80 deg. (Figure 1). The angle of inclination of the cell was 9 deg. 44 min. for this study. Data were taken at liquid Reynolds numbers of 732, 1,099, 1,482, and 1,834. The water temperature was 22.2°C.

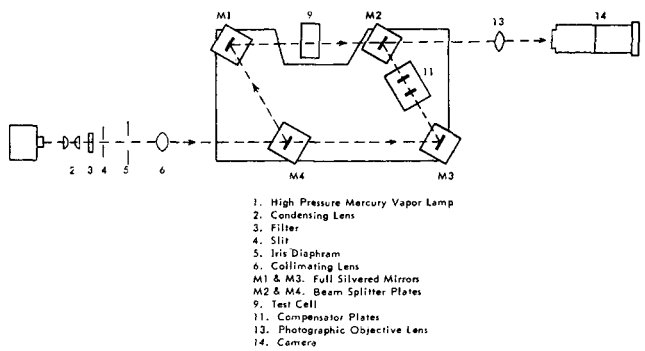

Fig. 1. Schematic diagram of interferometer.

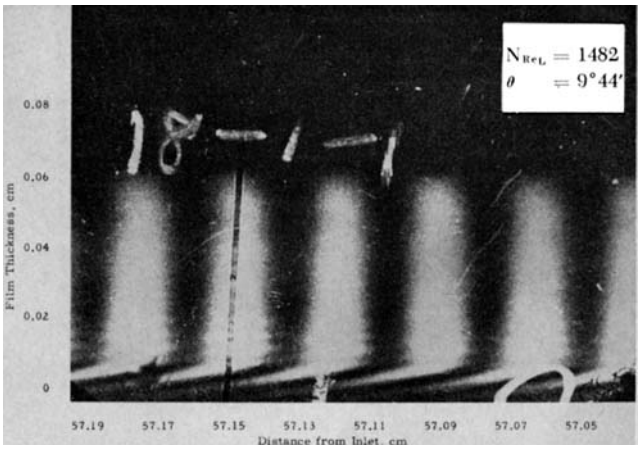

Fig. 2. Photograph of air–water interference pattern.

The position of interference fringes which appeared within the water film perpendicular to the bottom plate was photographed first with air above the water (to act as a reference point) and then with carbon dioxide. The position of a fringe relative to its position with no carbon dioxide present was a direct measure of its concentration averaged across the width of the cell. Distilled water flowed down the plate from a constant head-temperature (±0.05°C.) system. The water entered the cell through a slot located at the top edge of the glass plate. Carbon dioxide entered and discharged through slots located in the top plate of the cell. When the cell was purged, the gas discharge line from the cell was closed and the cell was maintained under a slight positive pressure (≅ 0.3 mm. Hg gauge).

With a spider web used as a reference line, the shift in the fringe pattern from air–water to carbon dioxide–water system was determined from the photographs. The absolute concentration was calculated from the relationship

$$\frac{C}{C_s} = \frac{\Delta N}{\Delta N_s} \qquad (1)$$

Photographs of the interference pattern in the liquid film were made with a magnification ratio of about 22 and enlarged to a ratio of 119. With this magnification the error in determining the concentration near the interface was ±2%; the error increased to ±12% at the bottom of the film. This corresponds in absolute concentration to an error of about ±0.007 g./liter. Figure 2 shows a typical fringe system for air-water, and Figure 3 illustrates the same conditions when carbon dioxide had replaced air in the cell. The difference in the film thickness is a result of different amplitude waves being present when the photographs were taken. Changes in concentration were measured to within 0.1 mm. of the surface of the bottom plate and 0.02 mm. of the apparent gas-liquid interface. The thickness of the film at the time each photograph was taken was determined from the photograph.

Average carbon dioxide concentrations in the liquid leaving the cell was determined by chemical analysis.

Measurements of Wave Data

The behavior of the surface of the falling film and its thickness was determined by measuring the change in capacitance of the air gap between the surface of film and a copper strip 1/8 in. × 3/16 in. oriented so that its long axis was perpendicular to the direction of flow. The change in capacitance was measured by a capacitometer similar to that of Dukler and Berglin (*12*). The output from the capacitometer was recorded on a visicorder, at a chart speed of 1 in./sec. Measurements were made 80 cm. from the water inlet to the cell

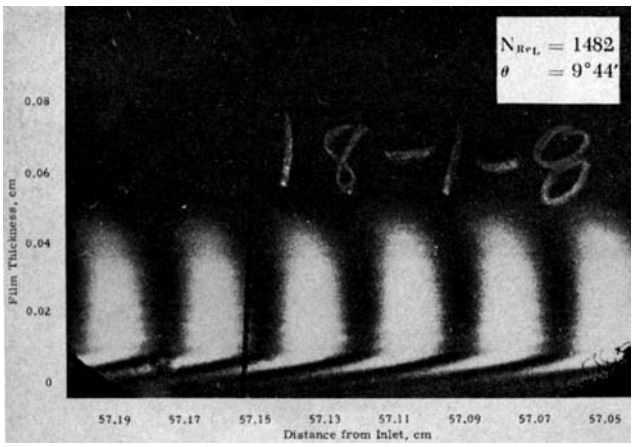

Fig. 3. Photograph of carbon dioxide–water interference pattern.

at angles of inclination of 9 deg. 44 min., 18 deg. 27 min., and 25 deg. 42 ft. The liquid flow rates were the same as those used in the mass transfer studies.

ANALYSIS OF THE EXPERIMENTAL DATA

Wave Data

The most readily measurable characteristics which describe the wave phenomena that occur on the surface of the liquid film are the Reynolds number, the wave frequency, and the wave amplitude.

Inspection of the wave traces revealed that both the amplitude and frequency of the waves were of a random nature and could be characterized by a statistical correlation. A distribution function P_A was defined as the ratio of the number of waves having a film thickness equal to or less than a given film thickness divided by the total number of waves observed. The value of P_A was unity at the maximum film thickness observed and zero at the minimum. When one utilizes the probit method (*1*), the wave amplitude data were found to be represented by a logarithmic normal distribution:

$$d\Phi_a(t) = d\psi\left(\frac{\ln t - \chi}{\sigma}\right) = \frac{1}{\sqrt{\pi\sigma}} \exp\left[\frac{-(\ln t - \chi)^2}{2\sigma^2}\right]\frac{dt}{t} \quad (2)$$

where $M(\ln x) = \chi$ is the mean, and $\sigma(\ln x) = \sigma$ is the dispersion. The correlation of the wave frequency data was made in a similar manner. With an arbitrary time interval of 1 sec. chosen, the number of waves per time interval was determined. A probability P_W was defined as the ratio of the number of time intervals having a wave frequency less than or equal to a given wave frequency divided by the total number of intervals. As in the amplitude data, the probability P_W was equal to unity at the maximum frequency observed and zero at the minimum. Again from the probit method, it was found that the wave frequency data were correlated by the normal distribution:

$$d\Phi_a(t) = \frac{1}{\sqrt{\pi\sigma}} \exp\left[-\frac{(t-\chi)^2}{2\sigma^2}\right] dt \quad (3)$$

The antilogs of the wave amplitude logarithmic normal mean YMF, the wave frequency normal means ω, and the average trough heights YT are given in Table 1.

Table 1. Velocity and Area Measurements, θ = 9 Deg. 44 Min.

N_{Re_L}	Y_L, cm.	V_{SL}, cm./sec.	$2V_A$, cm./sec.	Y_{MF}, cm.	ω, sec.$^{-1}$	V_{SMF}, cm./sec.	Y_T, cm.	Percent increase in surface area
732	0.067	39.3	52.4	0.092	5.9	73.4	0.042	1.4
1,099	0.077	51.0	68.0	0.096	8.3	80.9	0.052	1.2
1,482	0.085	62.3	83.3	0.098	13.1	84.1	0.060	1.7
1,834	0.091	71.6	95.6	0.107	15.8	91.8	0.064	2.3

Surface Area

The visicorder wave traces were plots of the location of the surface of the film for a given cell position as a function of the velocity of the waves and the visicorder chart speed. To calculate the surface area, the relationship between the visicorder chart speed and the velocity of the waves had to be known. The velocity of the waves was assumed to be equal to the surface velocity of an equivalent laminar film: $V_{wave} = V_S = 3/2\ V_A$. The use of 3/2 V_A for the velocity of the waves was not correct, as it has been experimentally determined (*20*) that the surface velocity of such films was closer to $2V_A$, and from hydrodynamic considerations the velocity of the waves should be at least equal to the surface velocity. The 3/2 V_A, however, overestimated the area, thus insuring that the estimated increase in area was a maximum, thus maximizing the effect on the mass transfer rate. Results of the evaluation of surface area are given in Table 1.

The measured increase in surface area as a result of waves is about a factor of 10 smaller than that reported by Tailby and Portalski (*35*). This discrepancy may be a result of two basic differences in the experimental system. The first is that the cell width used in this work was 3 in., whereas Tailby's plate was 21 in. in width. The second difference is the angle of inclination of the cell. In this work, the angle of inclination was 9 deg. 44 min., whereas Tailby used a vertical plate.

Wave Model

To be able to calculate the average carbon dioxide concentration in the film from the interferometric data, to estimate a reasonable velocity profile, and to calculate values for the eddy diffusivity, we required a model of the film. The following model was used.

The film was divided into two regions. The first was a homogeneous region consisting of that part of the film from the surface of the bottom glass plate to the average trough height (Y_T) determined from the visicorder traces. The second region was that part of the film from the average trough height to the surface of the film. The waves were assumed to be triangular in shape with a uniform height defined by the mean film thickness (Y_{MF}) determined from the statistical correlation of the wave amplitudes. The mean film thickness Y_{MF} was considered to be the maximum height of the waves and Y_T the base of the waves in the analysis of the experimental data. The number of waves in a 1-sec. time interval was set equal to the mean wave frequency also determined from the wave data. The velocity profile in the film was assumed to be parabolic in shape (*37*) and was set equal to the velocity profile [Equation (*4*)], calculated by assuming a laminar film of thickness Y_{MF} flowing at the same angle of inclination (θ). With this assumed velocity profile the velocity of the liquid in the waves was calculated as though the waves were not present and the liquid was flowing as a laminar film:

$$V(Y) = \frac{\rho g \sin\theta\,(Y_{MF})^2}{2\mu}\left[1 - \left(\frac{Y_{MF} - Y}{Y_{MF}}\right)^2\right] \quad (4)$$

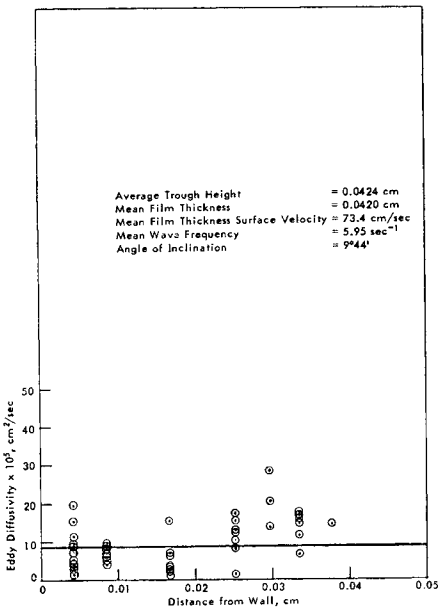

Fig. 4. Calculated eddy diffusivities for Reynolds number = 732.

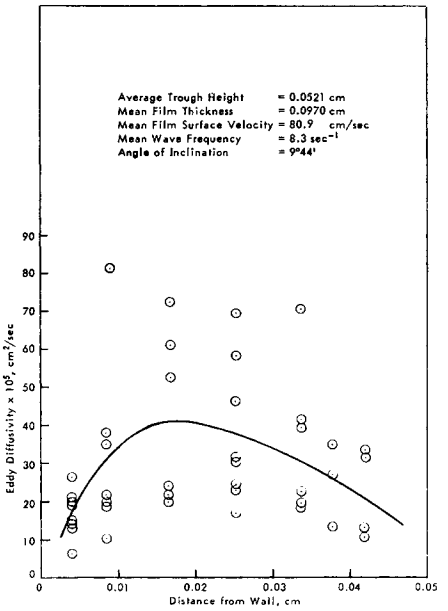

Fig. 5. Calculated eddy diffusivities for Reynolds number = 1,099.

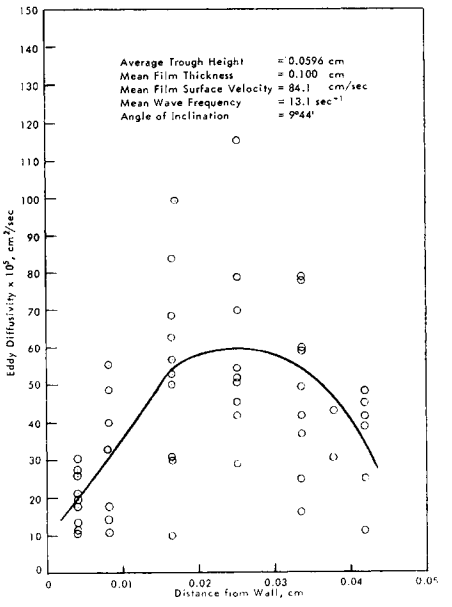

Fig. 6. Calculated eddy diffusivities for Reynolds number = 1,482.

where $0 \leqq Y \leqq Y_{MF}$. The use of Equation (4) to describe the velocity profile is appropriate as μ/ρ is much greater than the measured eddy diffusivities. The width of the triangular waves at the average trough height was determined by assuming a base width and calculating the total mass flow rate. The correct width was determined when the calculated flow rate equaled the measured flow rate. This model of the flow of the film with waves appeared reasonable when compared visually with the corresponding wave traces.

Evaluation of the Eddy Diffusion Coefficients

Mass transfer in the flowing film was assumed to be described by the equation

$$V(Y)\frac{\partial C}{\partial Z} = \frac{\partial}{\partial Y}\left((D+\epsilon)\frac{\partial C}{\partial Y}\right) \tag{5}$$

When one chooses as a system a rectangularly shaped increment of water of unit width, length $Z_2 - Z_1$, and thickness Y, the molecular species balance was

$$-(Z_2 - Z_1)(D+\epsilon)\frac{\partial C}{\partial Y}\bigg|_{\frac{Z_1+Z_2}{2}} = \int_0^Y V(Y)C(Y)dY\bigg|_{Z_2} - \int_0^Y V(Y)C(Y)dY\bigg|_{Z_1} \tag{6}$$

When one solves for $(D+\epsilon)$ and substitutes in Equation (4) for the velocity profile Equation (6) becomes

$$D+\epsilon(Y) = \frac{-V_s}{Z_2 - Z_1}\left(\frac{\partial Y}{\partial C}\right)_{\frac{Z_1+Z_2}{2}} \left[\int_0^Y \left\{1-\left(\frac{Y_{MF}-Y}{Y_{MF}}\right)^2\right\} C(Y)\,dY\bigg|_{Z_2} - \int_0^Y \left\{1-\left(\frac{Y_{MF}-Y}{Y_{MF}}\right)^2\right\} C(Y)\,dY\bigg|_{Z_1}\right] \tag{7}$$

where

$$V_s = \frac{\rho(Y_{MF})^2 g \sin\theta}{2\mu}$$

To eliminate entrance effects, Equation (7) was evaluated by assuming that the concentration profile at $Z = 57.15$ cm., well beyond the wave inception point, was the initial profile. Values of the integral were determined by graphical integration where $C(Y)$ was the concentration profile as determined from the interferometric data. Values of dY/dC were also obtained from the concentration profiles by fitting the data with a fourth-order polynomial and by differentiating the resulting equation. In the case where more than one set of data was available at a given cell position and flow rate, the value of $C(Y)$ and dY/dC used was the average values of the data available. Results of these evaluations are given in Figures 4, 5, 6, and 7. The solid line drawn through the points represents the arithmetic mean for each set of points.

DISCUSSION

Wave Hydrodynamics

The surface profile of the falling films as recorded by the visicorder showed that when ripples first formed on the surface of a falling film ($N_{Re} = 8$), they were of a fairly uniform frequency and amplitude. As the liquid flow rate was increased, the frequency and amplitude of the waves became irregular. The effect of increasing the angle of inclination of the cell while maintaining the same liquid flow rates was to decrease the film thickness and change the flow pattern. There was no apparent pattern to the change of the mean wave frequency with the angle of inclination of the cell.

The effect of the wall on the shape of the waves as they moved down the plate was not measured with the capacitometer. However, visual observations indicated a retarding of the velocity of the waves at the wall with the long axis of the wave being generally perpendicular to the direction of flow at the center of the plate and slightly bowed at the walls. The waves were always continuous across the width of the cell.

MASS TRANSFER RESULTS

Visual Observations

The most successful feature of the experimental technique was the presentation of actual concentration profiles in a system where they fluctuate because of waves. Motion pictures would be the most effective description; however,

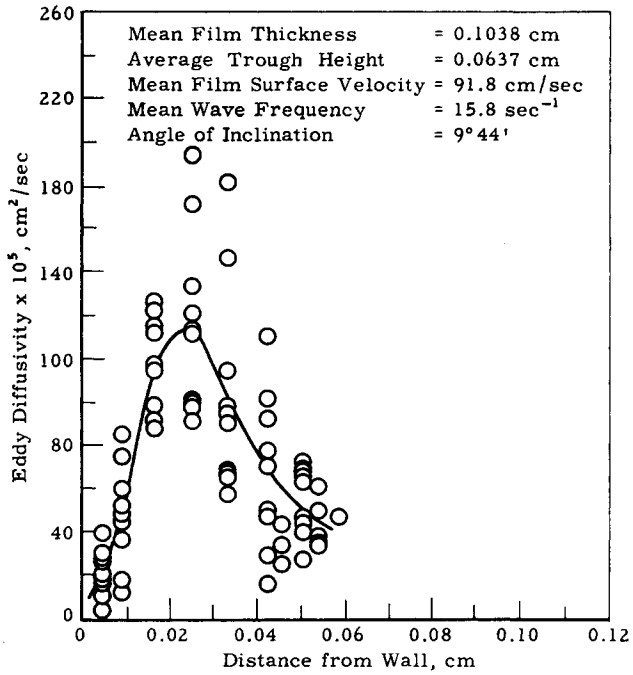

Fig. 7. Eddy calculated eddy diffusivities for Reynolds number = 1,834.

certain important features can be described. Visual observations of the interference pattern in the cell in the region next to the water inlet when carbon dioxide was being absorbed indicated that mass transfer in this region was by molecular diffusion. However, as the liquid moved down the cell, the film accelerated, became unstable, and formed waves. As soon as the waves appeared, the rate of absorption of carbon dioxide into the film increased. The shape of the interference pattern near the interface did not change significantly with the appearance of the waves, but the shift of the pattern near the bottom indicated that the carbon dioxide penetrated rapidly to the bottom of the film. As the film moved further down the plate, the interference pattern near the bottom continued to shift, showing that the concentration was increasing. However, the orientation of the interference pattern in this region with respect to the reference line changed very little from the air-water orientation, indicating a very small concentration gradient in the film. A comparison of these observations with the concentration profile predicted by assuming a laminar film with molecular diffusion shows that the increase in concentration at the bottom of the film was much greater than predicted and the concentration gradient much smaller. For this to be true, some dynamic action or turbulence in the central region of film must be aiding the diffusion. The observation that almost no concentration gradient existed in the film near the bottom indicates that turbulence may exist near the bottom.

The effect of the waves on the concentration profile in the region below the average trough height was negligible. The concentration profile was the same whether a large wave or trough was passing over the point of observation. In the film above the average trough height the following characteristics were observed. The concentration near the surface of the waves appeared to be nearly constant regardless of the film thickness. As the waves moved past a given point in the cell, the interference pattern, proportional to the concentration profile, was compressed and expanded following the surface of the film as produced by the waves. Figure 8 shows some experimental concentration profiles obtained at the same cell position, angle of inclination, and liquid flow rate for different film thicknesses which result as waves pass the camera. In all cases, it was found that for a particular cell position and liquid flow rate, a concentration profile measured at a given wave amplitude could be superimposed upon profiles for other wave amplitudes by proportionally expanding or contracting the film thickness scale of the experimental curve to the observed film thickness. Because the concentration profiles for a particular liquid flow rate were all similar, a dimensionless length was used for the film thickness in the mass transfer equation even though the film thickness varied.

Determination of Eddy Diffusivities

Calculation of the eddy diffusivity in the bulk of the film was based on Equation (7). The value of the integral in Equation (7) was obtained by graphical methods, and the velocity profile used was that based on the mean film thickness [Equation (4)]. Figures 4, 5, 6, and 7 show the results of this analysis. The solid line represents the arithmetic mean of each set of points. Although the data scatter, the effect of location in the film and the liquid flow rate is readily apparent. Diffusivities shown are calculated from data taken at distances ranging from 57.15 to 82.5 cm. from the inlet. Evaluation of the diffusivities were made at values of $Z_2 - Z_1$ between 6.35 and 25.35 cm.

The scatter in the calculated diffusivities is the result of a varying film thickness resulting in the expansion and compression of the concentration profiles with the passage of a wave. This caused the slope of the concentration profile at a particular location in the film to change with time, whereas the fringe location (below the base of the waves) remained constant. This in turn resulted in some scatter in the value of the integral but more importantly caused as much as a twofold fluctuation in the slope. This error could have been minimized if all the experimental data had been taken at the same film thickness, as for instance only when a crest of a wave was passing. However, this proved too difficult experimentally. Values of the diffusivity were obtained only for that part of the liquid film which was below the average trough height. No attempt was made to determine the value of the diffusivity above the average trough height, as the variable film thickness resulting from the presence of waves caused too much

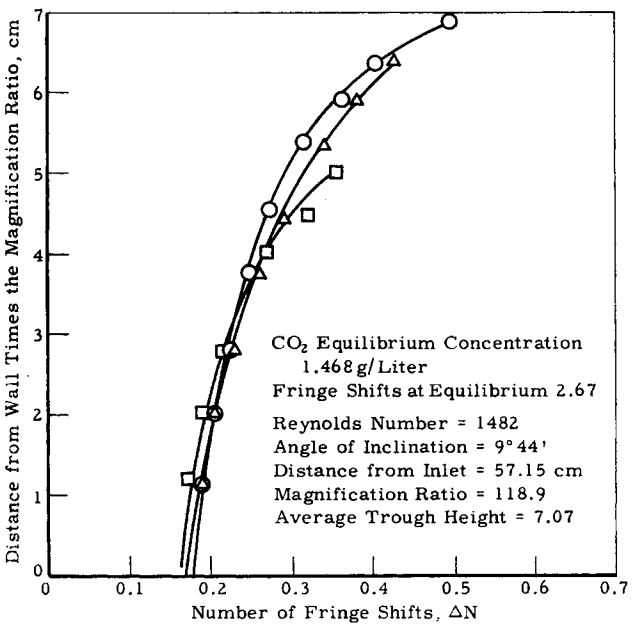

Fig. 8. Effect of waves on the concentration profile.

scatter in the slope of the concentration profile. It should be emphasized that, from visual observations and from data obtained on the concentration profile in the upper half of the waves, the scatter in the slope of the concentration profile was presumably the result of comparing data at different film thicknesses and was not the result of any relatively large eddies in the film.

Figure 9 is a plot of the arithmetic mean values of the diffusivities for each location in the film as a function of the liquid flow rate. It can be seen that the magnitude of the diffusivity in the film varies considerably with location in the film and the liquid flow rate. The eddy diffusivity is a maximum in the center of the film and decreases as the bottom plate and interface are approached with the diffusivity increasing as the liquid flow rate is increased. At a Reynolds number of 732 the dependency of the diffusivity on location in the film does not appear to be significant. The decrease of the eddy diffusivity in a falling film as the bottom plate and interface are approached is interesting as it offers an explanation for the mechanism of mass transfer when ripples form on the surface of the film and there is little increase in surface area. With reference to Table 2, which gives values of the pseudo diffusivities calculated in a manner similar to that suggested by Stirba and Hurt (*34*), it can be seen that these apparent diffusivities are much smaller than the experimental diffusivities. Even if surface velocity and film thickness corresponding to the maximum wave height were used in this calculation, the value of the pseudo diffusivity would still be much smaller than the measured values.

These results indicate that some mechanism other than diffusion in the bulk of the film must be controlling the rate of mass transfer. It is proposed that this mechanism is the presence of a surface layer where eddy diffusivity approaches zero and the rate of mass transfer is controlled only by molecular diffusion. In extremely turbulent systems, this layer would be very small, while in the flow regime where waves form, but are well behaved, the layer would be much thicker.

Based on these observations, some comments can be made on the various theoretical models. The surface renewal models of Danckwerts (*11*) and Harriott (*18*)

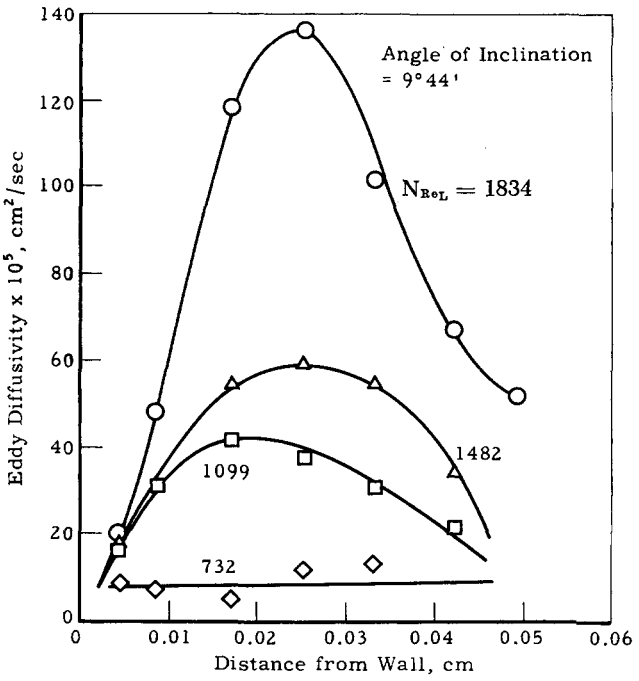

Fig. 9. Effect of liquid flow rate and location in the film on the averaged eddy diffusivity.

TABLE 2. COMPARISON OF PSEUDO DIFFUSIVITIES WITH EXPERIMENTAL DATA

N_{Re_L}	θ	$D_1 \times 10^5$, sq. cm./sec.	$D_2 \times 10^5$, sq. cm./sec.	$D_3 \times 10^5$, sq. cm./sec.
732	9 deg. 44 min.	2.20	3.52	~8
1,099	9 deg. 44 min.	2.30	3.87	~15-40
1,482	9 deg. 44 min.	2.26	4.05	~15-55
1,834	9 deg. 44 min.	1.34	5.34	~20-120

D_1: pseudo diffusivity, includes entrance effect.
D_2: pseudo diffusivity, no entrance effect.
D_3: experimental values.

could be used to evaluate the experimental data. However, evaluation of the parameters which describe the eddy age and distances from the interface which the eddies penetrate is not straightforward, and as a result it was felt that evaluation of the data in terms of an eddy diffusivity would be more meaningful. The validity of this method of interpretation of the experimental data should not be questioned because of the scatter in the calculated diffusivities until more experimental data is available and the effect of the variable film thickness can be further evaluated. Brauer's assumption (*7*) that a laminar layer at the wall of the cell controls the rate of mass transfer is incorrect in that in the case of absorption of a gas into the liquid film the laminar or stagnant layer exists at the free interface. This point, however, is academic; in the development of his model the existence of a laminar layer is proposed, but its location is not specified in the resulting equations. The pseudo diffusivity model of Stirba and Hurt (*34*), which was discussed earlier, also is apparently in error because of the assumption that the diffusivity does not vary with location in the film. The last model discussed, Levich's turbulent film model (*27*), appears to be the most accurate. The laminar film model is not correct because it does not allow turbulence in the bulk of the film. However, the turbulent film model appears generally to describe the experimental results for both laminar and turbulent flow in that it does predict that the eddy diffusivity is a maximum in the center of the film and decreases as the wall and free interfaces are approached. It might be said that the old Whitman two-film theory, which utilizes a well-mixed core in the fluid film, is not inappropriate. However, it does require a molecular diffusion process throughout a film of finite thickness.

The question as to how the hydromechanics which cause the waves contribute to the increase in diffusivity in the central region of the film has not been answered. The concentration profiles in the wave are not suddenly dispersed as a dye would be by the onset of turbulent flow, but merely stretched and compressed. The hydromechanical theory which adequately explains much of the wave character does not contain elements which allow a local irreversible mixing such as one has in turbulent flow. In accordance with Portalski (*31*), the presence of the secondary flow available from a modification of the linear theory of Kapitsz could cause the effect. On the other hand, the studies in flow visualization of Runstadler and Klein (*25*) suggest that turbulent eddies produced by the boundary-layer flow across the bottom plate would travel into the central region of the film and possibly control the thickness of a laminar layer at the surface.

CONCLUSIONS

It has been shown that waves in a falling liquid film increase the rate of mass transfer by as much as 50 to 100%. The increase in surface area is no more than 2.5%

for the flow rates used and cannot account for such high mass transfer rates. Calculation of eddy diffusivities in the film indicates that as the flow rate is increased, the diffusivity in the film is increased and a maximum diffusivity occurs in the central region of the film. As the interface and bottom plate are approached, the value of the eddy diffusivity decreases and seems to tend toward the molecular diffusivity. Molecular diffusion through a quiet or laminar film next to the interface seems to control the rate of mass transfer.

The effect of waves on the concentration profile is to compress and expand the profile with the concentration near the interface remaining constant. These results indicate that the waves do not have a direct effect on rate of mass transfer in the film but are a result of, perhaps, the same mechanism that controls the diffusivity. The amplitude and frequency of the waves did not appear to be the correct variables to use in correlating the eddy diffusivity.

ACKNOWLEDGMENT

The authors gratefully acknowledge financial support of this work by National Science Foundation Grants G-9698 and GF-527.

NOTATION

C = concentration of carbon dioxide in water, g./liter
C_s = saturation concentration of carbon dioxide in water, g./liter
D = diffusion coefficient, sq. cm./sec.
g = acceleration of gravity, cm./sec.^{2}
$M(\ln x) = \chi$ = mean or center of gravity of the whole probability mass
N_{Re_L} = Reynolds number of the liquid film, $4Q\rho/\mu$
ΔN = number of fringe shifts: distance a fringe shifts/fringe spacing
ΔN_s = number of fringe shifts that correspond to water saturated with carbon dioxide
P_A = wave amplitude probability
P_W = wave frequency probability
Q = volumetric flow rate per unit width of the cell, cc./(sec.)(cm.)
t = intervals in which the experimental observations were measured
V_A = bulk average film velocity, cm./sec.
V_S = surface velocity of the liquid film with waves, cm./sec.
V_{SL} = laminar film surface velocity, cm./sec.
V_{SMF} = surface velocity of a laminar liquid film of thickness Y_{MF}, cm./sec
V_{wave} = velocity of waves on the surface of the film, cm./sec.
Y = distance from the surface of the bottom plate of the contacting cell to some point in the liquid film, cm.
Y_L = laminar film thickness, cm.
Y_{MF} = mean film thickness calculated from the mean of probability mass describing the film thicknesses
Y_T = average trough height of the liquid film, cm.
Z = distance of gas-liquid contact, measured from the water inlet, cm.

Greek Letters

ϵ = eddy diffusivity, sq. cm./sec.
ϵ_m = maximum eddy diffusivity, sq. cm./sec.
μ = viscosity, poise
ρ = liquid density, g./cc.
σ = $\sigma(\ln x)$ dispersion or square root of the moment of inertia of the total probability mass
$\Phi_x(t)$ = theoretical distribution function
$\psi(t)$ = normalized distribution function $\chi = 0$ and $\sigma = 1$
ω = mean wave frequency, sec.$^{-1}$

Subscripts

i = location in the liquid film
T = location in the liquid film equal to the average trough height

LITERATURE CITED

1. Arley, Niels, and K. R. Buch, "Introduction to the Theory of Probability and Statistics," Wiley, New York (1950).
2. Bennett, F. D., *J. Appl. Phys.*, **22**, No. 2, 184 (1951).
3. *Ibid.*, No. 6, 776 (1951).
4. Binnie, A. M., *J. Fluid Mech.*, **2**, 551 (1957).
5. *Ibid.*, **5**, 561 (1959).
6. Belkin, H. H., et al., *A.I.Ch.E. J.*, **5**, 245 (1959).
7. Bauer, H., *Chem. Ing. Tech. NR 2*, **30**, 75 (1958).
8. Caldwell, C. S., Ph.D. thesis, Univ. Washington, Seattle (1955).
9. ———, J. R. Hall, and A. L. Babb, *Rev. Sci. Instruments*, **28**, No. 10, 816 (1957).
10. Cullen, E. J., and J. F. Davidson, *Chem. Eng. Sci.*, **6**, No. 2, 49 (1957).
11. Danckwerts, P. V., *I. E. C.*, **43**, No. 6, 1460 (1951).
12. Dukler, A. E., and O. P. Bergelin, *Chem. Eng. Progr.*, **48**, No. 11, 567 (1952).
13. Eckert, E. R. G., R. M. Drake, Jr., and E. Soehngm, *USAF Air Material Command Tech. Rept. 5747* (1948).
14. Emmert, R. E., and R. L. Pigford, *Chem. Eng. Progr.*, **50**, 87 (1954).
15. Friedman, S. J., and C. O. Miller, *I. E. C.*, **33**, No. 7, 885 (1941).
16. Garwin, Leo, and E. W. Kelly, Jr., *ibid.*, **47**, 392 (1955).
17. Grimley, S. S., *Trans. Inst. Chem. Engrs.*, **23**, 228 (1945).
18. Harriott, Peter, *Chem. Eng. Sci.*, **17**, 149 (1962).
19. Harvey, E. A., Ph.D. thesis, Univ. London, England (1958).
20. Jackson, M. L., *A.I.Ch.E. J.*, **1**, 231 (1955).
21. Johnstone, H. F., and R. L. Pigford, *Trans. Am. Inst. Chem. Engrs.*, **38**, 25 (1942).
22. Jepsen, J. C., Ph.D. thesis, Univ. Oklahoma, Norman (1964).
23. Kahl, G. D., and F. D. Bennett, *J. Appl. Phys.*, **23**, No. 7, 763 (1952).
24. Kamei, S., and J. Oishi, *Mem. Faculty Eng. Kyoto Univ.*, **18**, 1 (1956).
25. Kline, S. J., and P. W. Runstadler, Eng. Soc., New York; also *AFOSR-TNSZ41* (June, 1963).
26. Ladenburg, R. W., "High Speed Aerodynamics and Jet Propulsion," Vol. 9, p. 47, Princeton Univ. Press, N. J. (1954).
27. Levich, V. G., "Physiochemical Hydrodynamics," Chapt. Prentice-Hall, Englewood Cliffs, N. J. (1962).
28. Lin, C. S., R. W. Moulton, and G. L. Putnam, *I. E. C.*, **45**, No. 3, 640 (1953).
29. Lynn, S., J. R. Straatemeier, and H. Kramers, *Chem. Eng. Sci.*, **4**, No. 2, 49 (1955).
30. Malik, J. E., J. L. Speirs, and J. T. Rogers, *J. Chem. Education*, **30**, 437 (1953).
31. Nysing, A. T. O., and H. Kramers, *Chem. Eng. Sci.*, **8**, 81 (1958).
32. Portalski, Stanislaw, *I. E. C. Fundamentals*, **3**, 49 (1964).
33. Price, E. N., *Rev. Sci. Instruments*, **23**, No. 4, 162 (1952).
34. Stirba, Clifford, and D. M. Hurt, *A.I.Ch.E. J.*, **1**, No. 2, 178 (1955).
35. Tailby, S. R., and Stanislaw Portalski, *Trans. Inst. Chem. Engrs.*, **38**, 324 (1960).
36. Werner, F. D., and B. M. Leadon, *Rev. Sci. Instruments*, **24**, 121 (1953).
37. Wilkes, J. O., and R. M. Nedderman, *Chem. Eng. Sci.*, **17**, 177 (1962).
38. Willard, H. H., L. L. Merrit, and J. A. Dean, "Instrumental Methods of Analysis," Chapt. 8, van Nostrand, New York (1948).
39. Wirchler, John, *Rev. Sci. Instruments*, **19**, No. 5, 307 (1958).

Manuscript received January 18, 1965; revision received August 30, 1965; paper accepted September 1, 1965. Paper presented at A.I.Ch.E. Boston meeting.